1-2021

Wetting and Brazing of YIG Ceramics Using Ag–CuO–TiO2 Metal Filler

Wanqi Zhao
Harbin Institute of Technology, China

Shuye Zhang
Harbin Institute of Technology, China

Jian Yang
University of Science and Technology Beijing, China

Tiesong Lin
Harbin Institute of Technology, China

Dusan P. Sekulic
University of Kentucky, dusan.sekulic@uky.edu

See next page for additional authors

Wetting and Brazing of YIG Ceramics Using Ag–CuO–TiO2 Metal Filler

Digital Object Identifier (DOI)
https://doi.org/10.1016/j.jmrt.2020.12.080

Notes/Citation Information
Published in *Journal of Materials Research and Technology*, v. 10.

Authors
Wanqi Zhao, Shuye Zhang, Jian Yang, Tiesong Lin, Dusan P. Sekulic, and Peng He

Available online at www.sciencedirect.com

jmr&t Journal of Materials Research and Technology

journal homepage: www.elsevier.com/locate/jmrt

Original Article

Wetting and brazing of YIG ceramics using Ag–CuO–TiO_2 metal filler

Wanqi Zhao [a], Shuye Zhang [a,***], Jian Yang [b], Tiesong Lin [a,**], Dusan P. Sekulic [a,c], Peng He [a,*]

[a] State Key Laboratory of Advanced Welding and Joining, Harbin Institute of Technology, Harbin, 150001, China
[b] School of Materials Science and Engineering, University of Science and Technology Beijing, Beijing, 100083, China
[c] Department of Mechanical Engineering, College of Engineering, University of Kentucky, Lexington, KY, 40506, USA

ARTICLE INFO

Article history:
Received 21 August 2020
Accepted 22 December 2020
Available online 1 January 2021

Keywords:
Wettability
Ferrite devices
YIG ceramics
Ag–CuO filler
Brazing
$Y_2Ti_2O_7$ layer

ABSTRACT

The wetting and brazing of $Y_3Fe_5O_{12}$ (YIG) ceramics with a Ag–8CuO–2TiO_2 filler was investigated for the first time. For comparison, the wettability of a Ag–10CuO filler on YIG ceramics was similarly investigated. The Ag–8CuO–2TiO_2 filler has an equilibrium contact angle of approximately 31 °C on the YIG substrate at 1000 °C; thus, its wettability is excellent. Moreover, its wettability exceeds that of Ag–10CuO. The microstructure and the interfacial structure between the filler and the substrate were determined using scanning electron microscopy, X-ray diffraction, EPMA and transmission electron microscopy. The liquid Ag–8CuO–2TiO_2 filler can react with the YIG substrate by forming continuous $Y_2Ti_2O_7$ layers with dotted $CuFe_2O_4$ and promote the wetting behavior and bonding performance. The average shear strength could exceed 30 MPa for the joints at a brazing temperature of 1000 °C. As rupture occurred adjacent to the seam at the ceramic side, the strengths of the interfaces were characterized via nanoindentation. The hardness of the interface with doped TiO_2 exceeds that of Ag–10CuO, which is strengthened by the dotted $CuFe_2O_4$ among $Y_2Ti_2O_7$.

1. Introduction

YIG ceramics feature a series of attractive properties, such as low dielectric loss, a narrow resonance line width in the microwave region, and satisfactory saturation magnetization [1]. Therefore, they have been widely considered for use in tunable microwave devices (radar, telecommunication, and RF measurement systems) [2], circulators [3], isolators, phase shifters, tunable filters [4], and nonlinear devices [5]. However, YIG cannot be economically implemented if the manufacture of large and/or complex-shaped ceramic components is needed. Thus, the development of a suitable ceramic joining technology is essential. However, limited application of this

* Corresponding author.
** Corresponding author.
*** Corresponding author.
E-mail addresses: syzhang@hit.edu.cn (S. Zhang), hitjoining@hit.edu.cn (T. Lin), hithepeng@hit.edu.cn (P. He).
https://doi.org/10.1016/j.jmrt.2020.12.080

ceramic with state-of-the-art technologies [6–8] has been reported.

The currently used joining techniques are not necessarily satisfactory for such demanding applications. For example, adhesive bonding is used to join YIG ceramics due to its convenience, safety, and low cost [9,10]. However, neither organic nor inorganic adhesives possess sufficiently high thermal stability. Moreover, under a high load, insufficient thermal energy would not be released from the seam joint to the outside, thereby leading to inadequate heat transfer and an increase in the component's temperature beyond a tolerable level, which would ultimately lead to a decrease in YIG's magnetic characteristics. The adhesive seam joint generates voids/cracks [11]; thus, the shear strength of the joint decreases after a limited operating time following a thermal shock [12].

Soldering techniques are also widely used to join ferrite devices. The surface of ferrite must be premetallized before soldering can be conducted to increase the wettability of the solder over the substrate, but this premetallization lacks of metallurgical bonding. Moreover, soldered seams cannot effectively withstand elevated temperatures (solders have a low melting point), especially if the component must operate within high-temperature surroundings. The low strength of soldered joints limits their use in critical load-bearing structural components.

A new ceramic brazing technique, namely, reactive air brazing (RAB), has been widely used to join solid oxide fuel cells (SOFCs). Traditional brazing is often conducted in a reducing atmosphere at temperatures that exceed 800 °C (requiring rigorous hermeticity) [13]. However, RAB is conducted in an air atmosphere without special atmospheric requirements. The brazing filler metal that is used in RAB contains a noble metal and an oxide, which facilitates high-temperature oxidation resistance and metallic ductility and provides satisfactory oxide surface wettability [14]. The most widely used brazing filler metal in RAB is the Ag–CuO system. It has been used to join alumina [15], zirconia [16] and conducting membranes [17]. Depending on whether a substrate reacts with Ag–CuO, the matrix options may be divided into (i) reactive (alumina) or (ii) nonreactive (zirconia) [13]. For both reactive and nonreactive substrates, the addition of active oxide TiO_2 has been proven to enhance the wettability of Ag–CuO, thereby resulting in fewer joint defects [18,19].

The advantage of the innovative bonding of the proposed YIG ceramic is that the added TiO_2 improves the wettability of the Ag–CuO filler on $Y_3Fe_5O_{12}$ ceramics. No similar study has been reported on joining YIG ceramics by using Ag–CuO. The main hypothesis is that the addition of TiO_2 to the filler as the active oxide would improve the wettability of Ag–CuO on a YIG substrate at high temperature and improve the joint integrity. Evaluation of the validity of this hypothesis was the main objective of this study. A new mechanism for enhancing the wetting of the Ag–CuO filler system was identified via the addition of TiO_2.

2. Materials and experimental procedures

2.1. Materials

The YIG ceramic that was used in this study was provided in the form of a column (φ13 mm × 75 mm) by the CASIC 23rd Institute in Beijing, China. The microstructure and composition of the YIG ceramic, which are presented in Fig. 1(a) and (b), were obtained via SEM (FESEM, Quanta200FEG) and XRD (Philips X'pert, Holland), respectively. The YIG ceramic was cut into 5 × 5 × 3 mm blocks for brazing. The surfaces to be jointed were ground using a 1500# diamond abrasive disk and cleaned ultrasonically for 10 min with acetone before brazing.

The composite fillers were prepared by mixing Ag, CuO and TiO_2 powders, all with a mean particle size of ~50 μm. The composite fillers were milled for 4 h using a QM-SB planetary ball mill. All filler materials were purchased from Tianjiu Technology Co., Ltd. Changsha, China. The constituents of the composite fillers were (i) Ag–10CuO (at.%) and (ii) Ag–8CuO–2TiO_2 (at.%). The molar ratio of CuO and TiO_2 in Ag–8CuO–2TiO_2 was 4:1, at which the eutectic reaction between CuO and TiO_2 would occur at 919 °C to promote the fluidity of the filler [20]. The melting points of Ag–10CuO and Ag–8CuO–2TiO_2 were measured via differential scanning calorimetry (DSC, STA449F3, NETZSCH, Germany). As

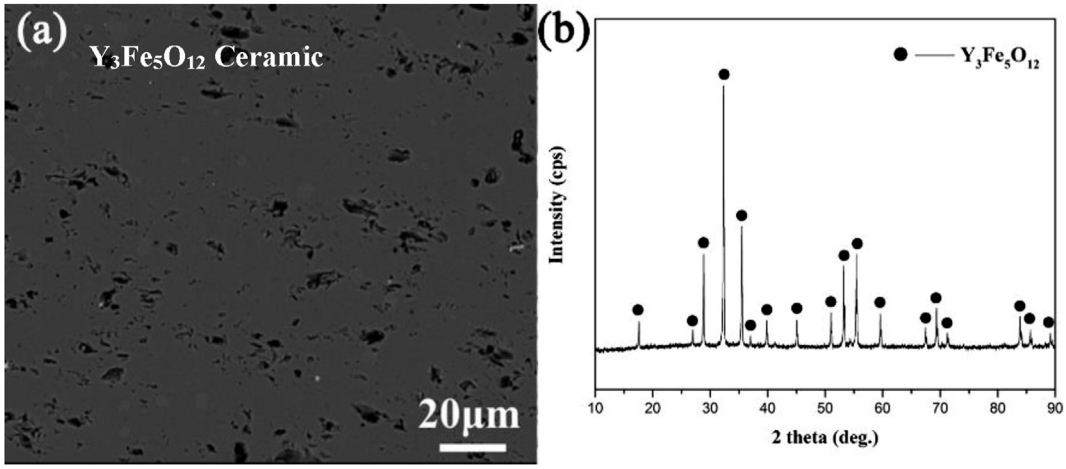

Fig. 1 – SEM (a) and XRD pattern (b) of YIG ceramic.

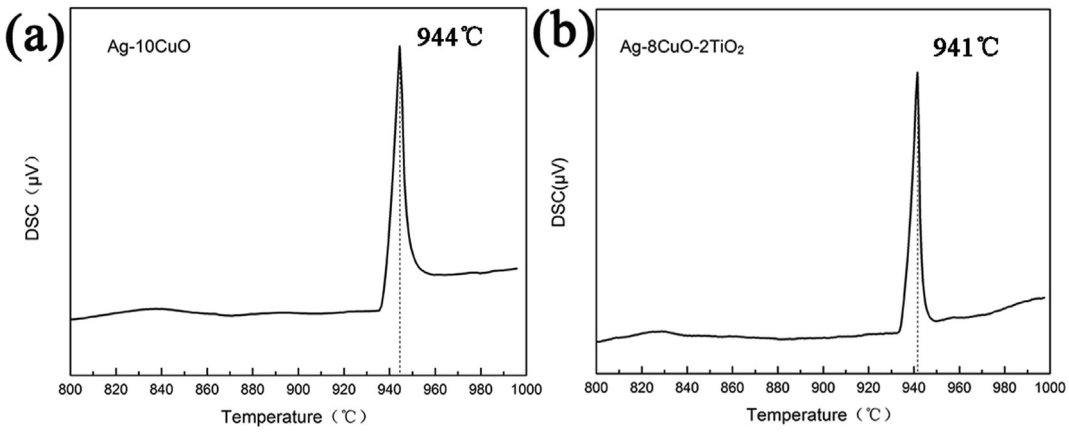

Fig. 2 – DSC curves of solders used for wetting and brazing: (a) Ag–10CuO, (b) Ag–8CuO–2TiO_2.

presented in Fig. 2, the melting point of Ag–8CuO–2TiO_2 is slightly lower than that of Ag–10CuO due to the eutectic reaction between CuO and TiO_2. The difference between the melting points could be ignored. The measurements were conducted in the temperature range of 20–1000 °C in air with a heating rate of 5 °C/min.

2.2. *Wetting experiments*

Wetting experiments were conducted using the technique of sessile drop spreading in real time in situ [21]. For these experiments, a Dataphysics OCA25-HTV1800 dynamic contact angle measurement system was used. The objectives were to visualize the spreading process and evaluate the kinetics of the triple line movement and to measure changes in the contact angle over time. The heating rate was 10 °C/min from 40 to 900 °C and 5 °C/min to the peak of 1000 °C with a holding time of 10 min. This was followed by cooling to room temperature (RT). The wetting angle was calculated via an ellipse fitting procedure using the software that was installed with the equipment. Cross-sections of the wetting samples after solidification were prepared to examine the wetting interface. The phases in the reaction layer were characterized via X-ray diffraction (XRD, Philips X'pert, Holland) with CuKα radiation (wavelength = 1.5418 Å) in the range of 2θ = 5–90°.

2.3. *Bonding experiment*

Bonding by brazing was conducted in air in a muffle furnace (KSL1400, Hefei Kejing Materials Technology Co., Ltd.). The heating cycle was implemented with temperature variations of less than ±5 °C. The slurry that was formed by mixing the filler and terpineol was dispensed on brazing surfaces by using a screen printing method to obtain a homogenous

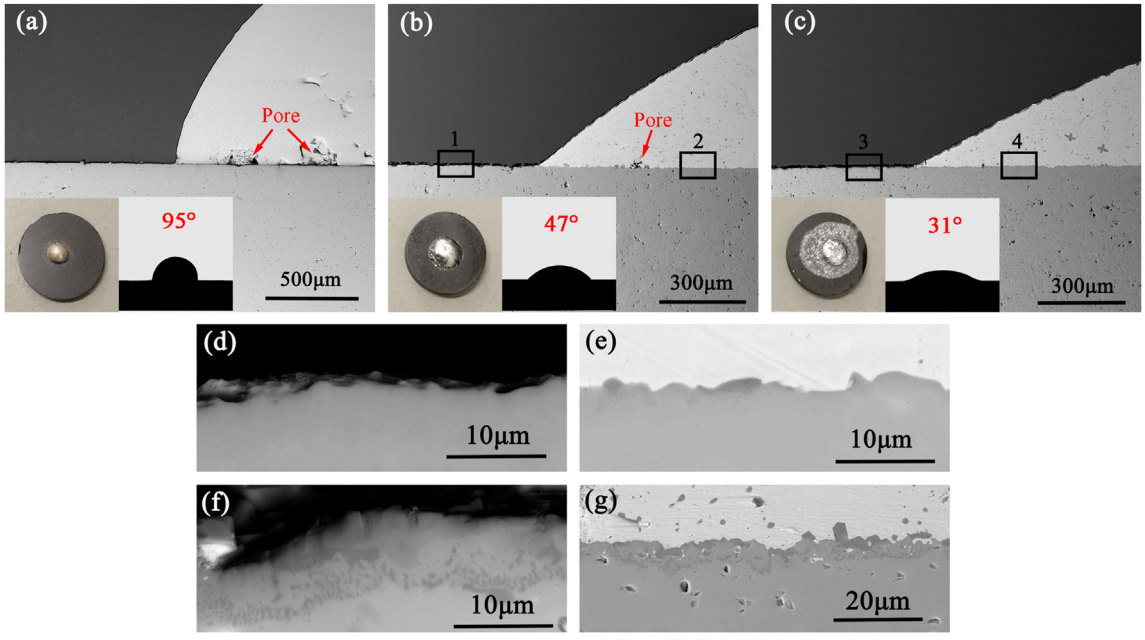

Fig. 3 – The equilibrium contact angles and interfaces obtained by different droplets at 1000 °C. (a) Ag; (b) Ag–10CuO; (c) Ag–8CuO–2TiO_2; (d), (e), (f) and (g) high magnification SEM observations of selected boxes 1, 2, 3 and 4.

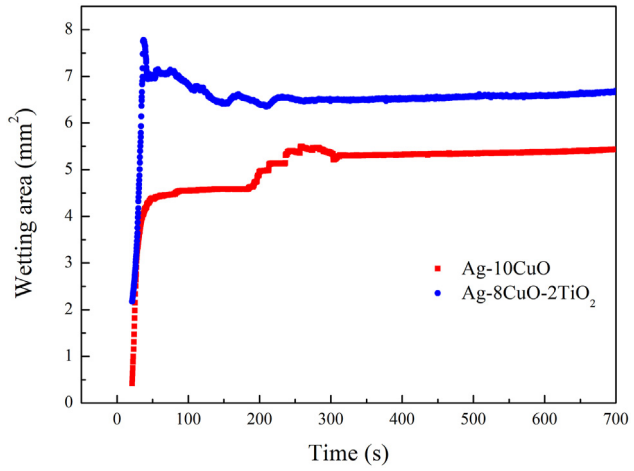

Fig. 4 – The variation of wetting area obtained by different droplets during the spreading process.

material distribution and uniform coating thickness. A pressure load of 2 kPa was applied on the brazing assembly to facilitate close contact between YIG mating surfaces. The heating rate was 10 °C/min. The brazed samples were cooled in the furnace via natural convection cooling to RT.

2.4. *Morphology and mechanical analysis*

The microstructure and chemistry of the wetting samples were investigated by using a scanning electron microscope (FESEM, Quanta200FEG) that was equipped with electron-dispersive spectroscopy (EDS) capability. A WDS analysis was conducted and an elemental distribution map of the brazed joint was obtained via electron probe microanalysis (EPMA, JXA-8230). The morphology and diffraction pattern of the reaction layer that formed adjacent to the YIG ceramic substrates were investigated via transmission electron microscopy (TEM, Talos F200X, FEI Co., Ltd, USA). The TEM specimen was prepared by utilizing a focused ion beam (FIB, Helios Nanolab 600i). Shear tests were conducted on a testing machine (Instron 5569) at room temperature with a constant speed of 0.5 mm/min. A nanoindentation test (continuous stiffness measurement) was conducted on a polished surface using a Nano Indenter G200 (Agilent) with a constant depth of 400 nm.

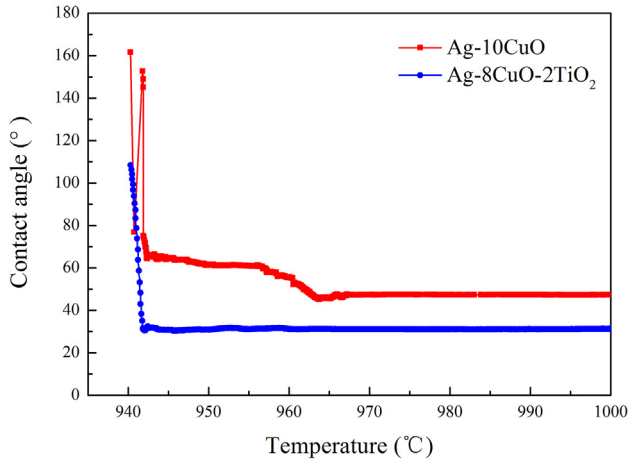

Fig. 5 – The variation of the contact angle along with the temperature.

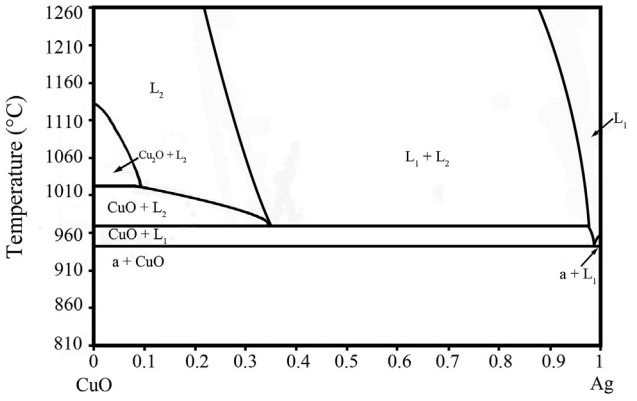

Fig. 6 – Ag–CuO phase diagram [14].

3. Result and discussion

3.1. *Wettability*

Fig. 3 shows the equilibrium contact angles and interfaces that were obtained using various filler constituents at 1000 °C. A smaller contact angle corresponds to better wettability [21,22]. The equilibrium contact angle of pure Ag on the YIG ceramic surface was 95°. Large pores were observed on the interface. The porosity would impact the mechanical integrity of the bond, and it is likely a combined consequence of gas phase formation at the surface and/or incomplete wetting, as presented in Fig. 3. When 10% mol CuO was introduced into the filler, the contact angle decreased dramatically to 47°. No reaction layer was readily identified at the interface, as shown in Fig. 3d–e. Dark-gray granular phases were found to form

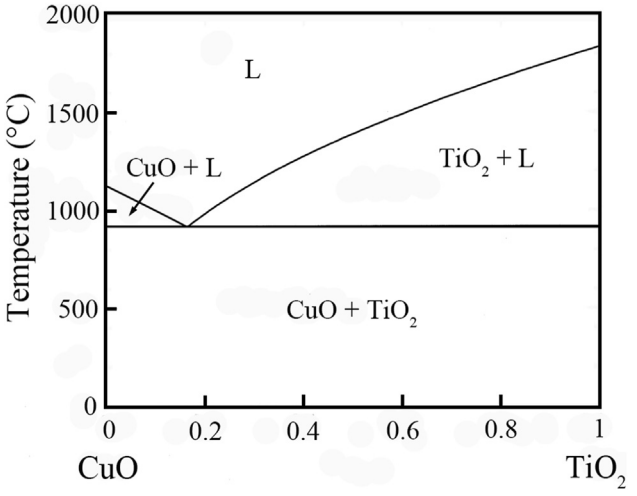

Fig. 7 – The calculated CuO–TiO2 phase diagram at $pO_2 = 1$ atm [20].

within the interphase domain, in addition to CuO. A further decrease in the contact angle from 47° to 31° occurred when 2 mol% TiO_2 was added to the filler. The filler in Fig. 3c was Ag–8CuO–2TiO_2; in this sample, we used 2 mol% CuO less than the amount that was used for Fig. 3b filler. A steady decrease in the contact angle with increasing CuO content relative to Ag over either a reactive or nonreactive substrate was expected [14]. We hypothesize that the decrease in the contact angle in Fig. 3c, instead of an increase, can be attributed to the addition of 2 mol% TiO_2, which may be the primary cause of the formation of a continuous reaction layer, as shown in Fig. 3f–g.

The spreading processes of the two fillers can be divided into two stages according to the wetting area variation [23], as shown in Fig. 4. With regard to Ag–10CuO, preliminary stabilization could be realized with a smaller area when the filler melted rapidly. Then, the droplet continued to spread until the time reached nearly 180 s, when it ultimately stopped spreading. As shown in Fig. 5, the second stage of the spreading process of Ag–10CuO was accompanied by a reduction in the contact angle when the temperature reached 957 °C.

The wetting phenomenon of Ag–10CuO can be explained by the occurrence of a monotectic reaction (Formula 1) between Ag and CuO when the temperature reaches nearly 960 °C [14]. When the temperature first reaches approximately 940 °C, L1 forms due to the eutectic reaction between Ag and CuO. As shown in Fig. 6, L_1 and L_2 are both liquid phases, which are both composed of Ag and CuO. L_2 is rich in CuO, whereas L_1 is rich in Ag. When the temperature is increased above 960 °C, more CuO dissolves into L_2 to form L_1. The formation of L_2 promotes wetting due to the increased concentration of CuO at the interface, which causes a secondary spreading process; this could be reflected in the change in the equilibrium contact angle.

$$L_2 \rightarrow L_1 + CuO \quad (1)$$

Moreover, with regard to Ag–8CuO–2TiO_2, according to the calculation of the CuO–TiO_2 phase diagram, which is presented in Fig. 7 [20], the molar ratio of CuO and TiO_2 in Ag–8CuO–2TiO_2 was 4:1, at which the eutectic reaction between CuO and TiO_2 would occur at 919 °C to promote the fluidity of the filler. The spreading process was irregular when the filler melted into a droplet, as shown in Fig. 4. The droplet moved rapidly around the initial position under the Dataphysics OCA25-HTV1800 camera. This left a wide reacted area around the solidified droplet, as shown in Fig. 3f. It is reasonable to posit that the addition of TiO_2 facilitated the interface reaction, which changed the inert YIG surface into

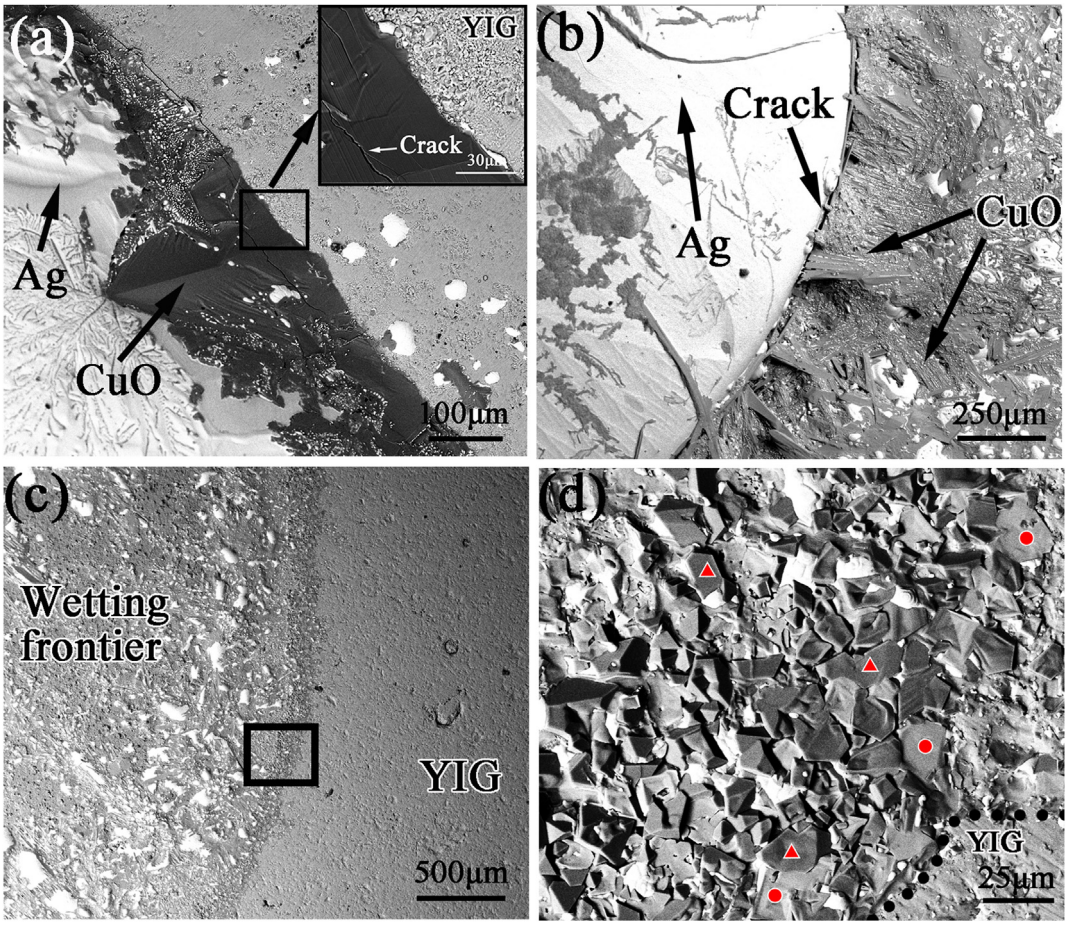

Fig. 8 – The top view of a solidified droplet's triple line vicinity area on YIG (a) the triple line of Ag–10CuO; (b) the triple line of Ag–8CuO–2TiO_2; (c) the wetting frontier area of Ag–8CuO–2TiO_2; (d) a magnified marked area in (c).

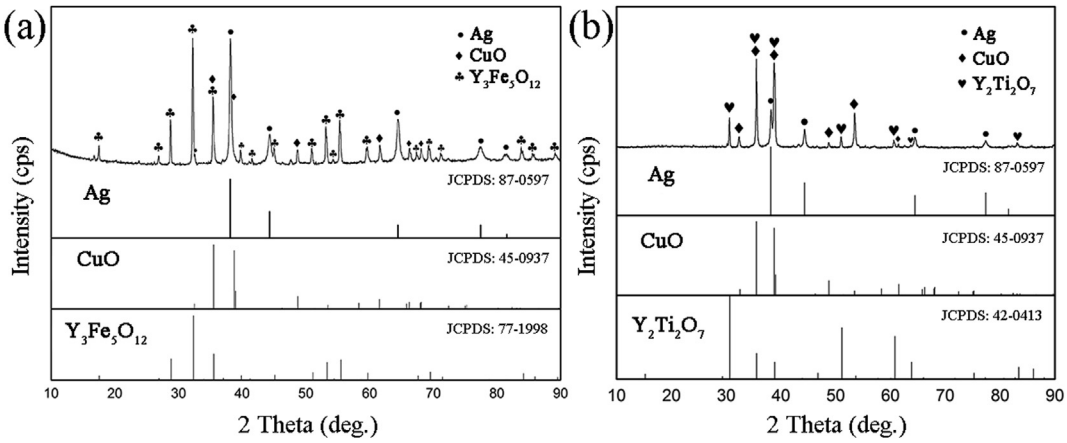

Fig. 9 – XRD profiles acquired from the surface of YIG wetted by (a) Ag–10CuO and (b) Ag–8CuO–2TiO_2.

an active reacted surface that could be doped with the active element Ti. As shown in Fig. 5, the contact angle of Ag–8CuO–2TiO_2 stabilized rapidly when the filler melted, without any readily observable change in the temperature. The spreading of the Ag–8CuO–2TiO_2 filler no longer depended on the dissolution of CuO into the liquid. The promotion of wetting by TiO_2 was substantially stronger than that by CuO.

3.2. *Morphological analysis*

To analyze the wetting behavior of Ag–10CuO and Ag–8CuO–2TiO_2 in more phenomenological detail, top views of the triple line zones of solidified droplets are presented in Fig. 8. The accumulation of CuO could be identified at distinct locations of the triple line of Ag–10CuO in Fig. 8a. The same could be observed for the Ag–8CuO–2TiO_2 wetting sample in

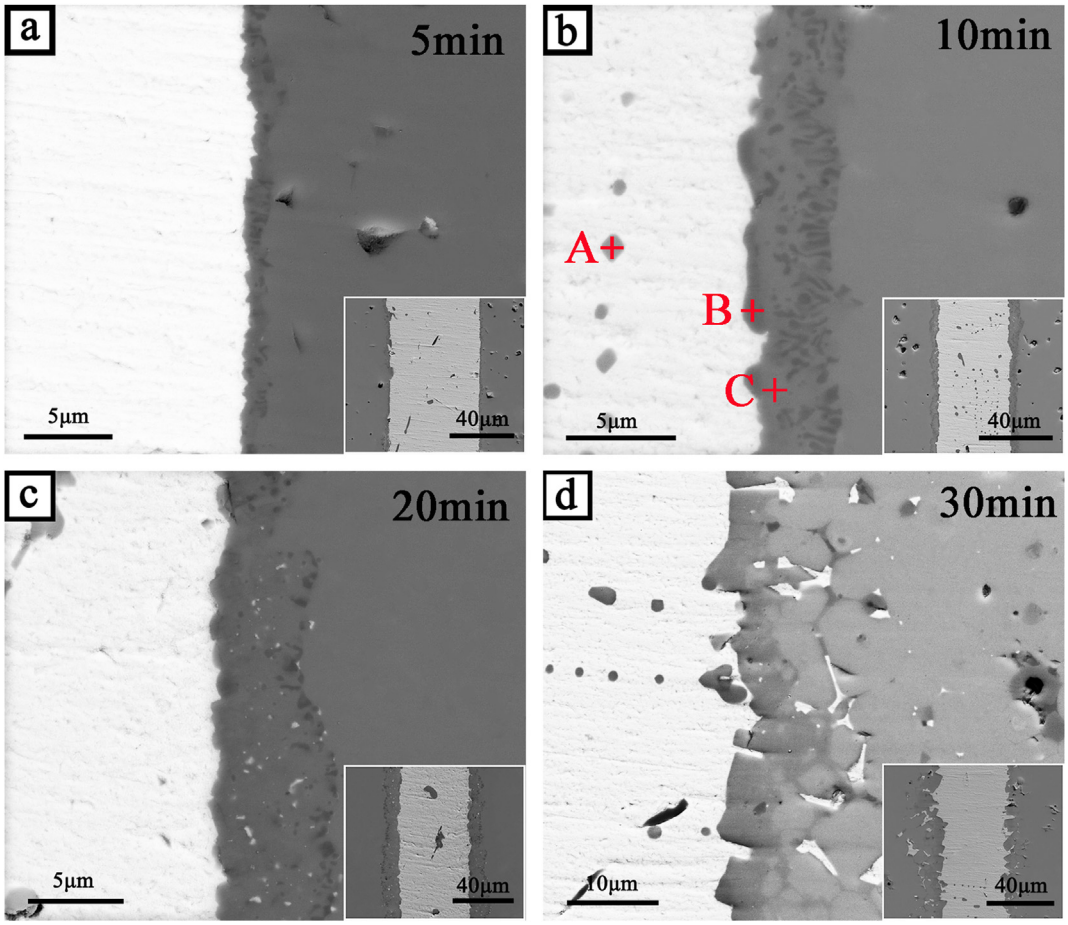

Fig. 10 – The interface of the YIG/YIG joints bonded by Ag–8CuO–2TiO2 at 1000 °C for (a) 5min (b) 10min (c) 20min (d) 30min.

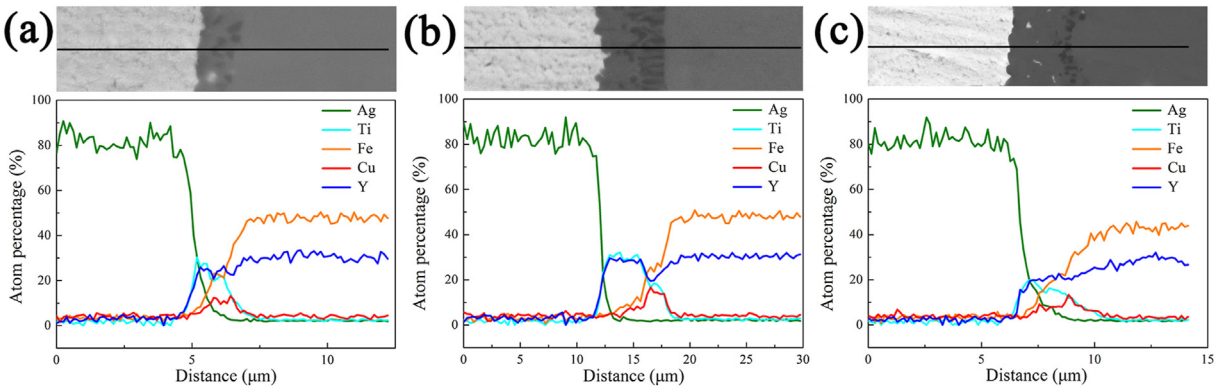

Fig. 11 – The linear scan results of typical interfaces of the YIG/YIG joints brazed by Ag–8CuO–2TiO_2 at 1000 °C for (a) 5min (b) 10min (c) 20min.

Fig. 8b. Although the increase in the CuO content improves the wettability, the brittleness of the joint in the vicinity of the interface would negatively impact the joint strength, especially if an increased quantity of CuO accumulates. Therefore, it is essential to control the amount of CuO. No other phases could be identified in the triple line domain of Ag–10CuO. The Ag–8CuO–2TiO_2 molten spread propagates rapidly and leaves an exposed reacted region at the interface. As shown in Fig. 8c–d, a band of a concentrated dark gray granular phase is formed at the edge of the wetting frontier, which is represented by triangles in Fig. 8d. The dark gray granules were preliminarily determined to include Cu and Fe via EDS analysis. Light gray phase domains are also visible and represented by circles in Fig. 8d. This phase includes mainly Y and Ti, identified via EDS, and likely constitutes the continuous reaction layer shown in Fig. 3f. Therefore, we hypothesize that the excellent wettability of Ag–8CuO–2TiO_2 on YIG results from the reaction among CuO, TiO_2 and the YIG ceramic at the interface.

To evaluate the formulated hypothesis, we began by identifying the products of the reaction at the interface. The YIG - Ag–10CuO interface was examined via XRD. Before the XRD examination, the resolidified droplets were ground slightly to make the surface flat. As shown in Fig. 9a, Ag, CuO and $Y_3Fe_5O_{12}$ were clearly detected, and no other phases were identified. The results demonstrate a lack of reaction between Ag–10CuO and the YIG ceramic. The reaction between Ag–8CuO–2TiO_2 and YIG was also considered. The $Y_3Fe_5O_{12}$ ceramic beyond the wetted region was cut off by a diamond wire saw to eliminate the effect of its presence. In addition to Ag and CuO, the pyrochlore crystal structure of transition metal $Y_2Ti_2O_7$ was identified in Fig. 9b. When TiO_2 was added to the filler, a continuous reaction layer with a dotted gray phase was formed at the interface shown in Fig. 3f–g. The matrix of the reaction layer towards the filler was hypothesized to be $Y_2Ti_2O_7$, which was proven, as presented in Fig. 9b. The presence of the $Y_2Ti_2O_7$ layer lowers the surface energy of the YIG ceramic, which would promote the wetting of the Ag–CuO filler over the ceramic surface.

3.3. *Joining mechanism*

The YIG ceramics were joined by the Ag–8CuO–2TiO_2 filler at 1000 °C for 5, 10, 20 and 30 min, as shown in Fig. 10. When the

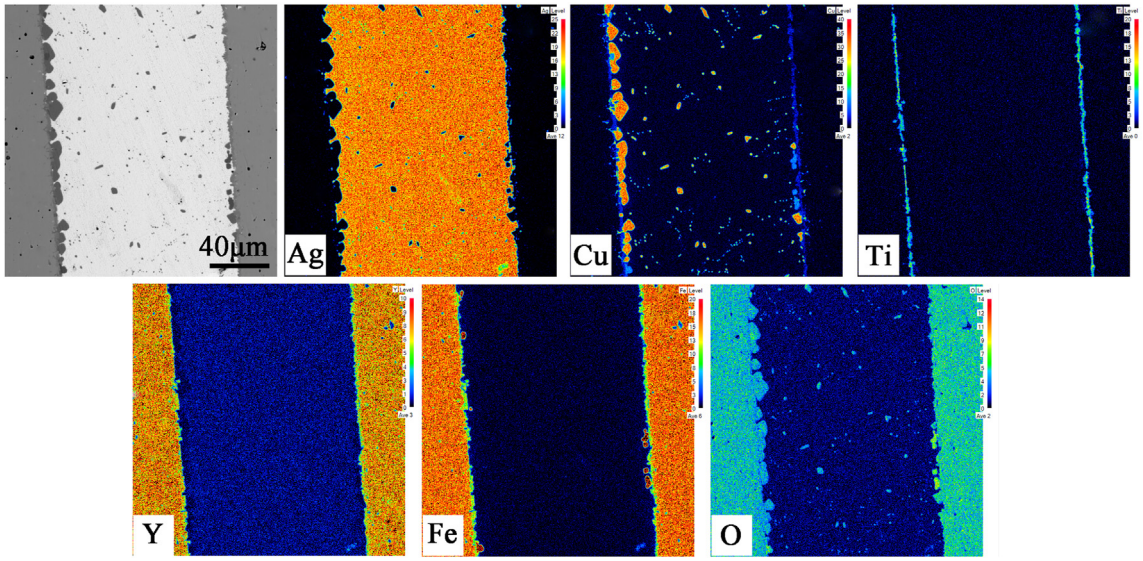

Fig. 12 – The EPMA maps of Ag, Cu, Ti, Y, Fe, O for the joint (1000 °C 5min).

Table 1 – WDS chemical analysis of different positions in Fig. 10(b) (at.%).

Phase Label	O	Y	Ag	Ti	Fe	Cu	Possible Phase
A	46.2	0	1.3	0.3	0.1	48.6	CuO
B	54.8	0.2	0.1	0.2	27.2	14.8	$CuFe_2O_4$
C	57.5	17.5	0.1	16.9	1.2	2.7	$Y_2Ti_2O_7$

holding time was 5 min, a continuous reaction layer was formed. WDS chemical analysis of different positions in Fig. 10(b) are shown in Table 1. The thickness of the layer was 2.5 μm; see the linear scan results in Fig. 11a. The reaction layer was clearly divided into two sublayers: one close to the filler with a molar ratio (1:1) of (Y: Ti) and the other near the YIG substrate with a molar ratio (1:2) of (Cu: Fe). The thickness of the reaction layer increased to 7.5 μm when the holding time was extended to 10 min. The dotted gray phase became much denser with larger phase domain sizes. When the holding time was increased to 20 min, Ag was distributed within the region of penetration into the YIG substrate. The dotted gray phase disappeared gradually from the interface with the diffusion of Ti and Cu to YIG, as shown in Fig. 11c. The homogenization of Ti and Cu within the domain was the primary cause of the disappearance of the dotted gray phase. The morphology of the interface became serrated when the holding time was increased to 30 min. This was most likely caused by severe intergranular penetration. No dotted gray phase could be identified at the interface under this condition. Fig. 12 shows the distribution of Ag, Cu, Ti, Y, Fe and O.

To further analyze the reaction mechanism between the Ag–8CuO–$2TiO_2$ filler and the YIG ceramic, TEM observations were conducted, and the results are discussed below. Fig. 13a presents bright-field images of the reaction layer that formed at 1000 °C after 10 min. According to the corresponding element distribution maps of the selected area in Fig. 13b, the dotted gray phase (marked as α) in the reaction layer was composed mainly of Cu and Fe, which was surrounded by a continuous phase (marked as β) that was composed mainly of Y and Ti. Selected-area diffraction techniques were used to determine the structures of the phases in the reaction layer, as shown in Fig. 13c–d. Phase α was proven to be cubic spinel $CuFe_2O_4$. Although the lattice spacing was slightly decreased due to slight displacement by Cu, phase β was proven to be pyrochlore $Y_2Ti_2O_7$, which was in satisfactory agreement with the XRD analysis results, which are presented in Fig. 9b.

3.4. *Mechanical properties*

The joints that were bonded by Ag–8CuO–$2TiO_2$ with various holding times were sheared, and the results are presented in Fig. 14c. Since the YIG ceramics are fragile, rupture occurs adjacent to the seam at the ceramic side, and the average strengths all exceed 30 MPa with no readily identifiable trend. The failure strength could not represent the strength of the

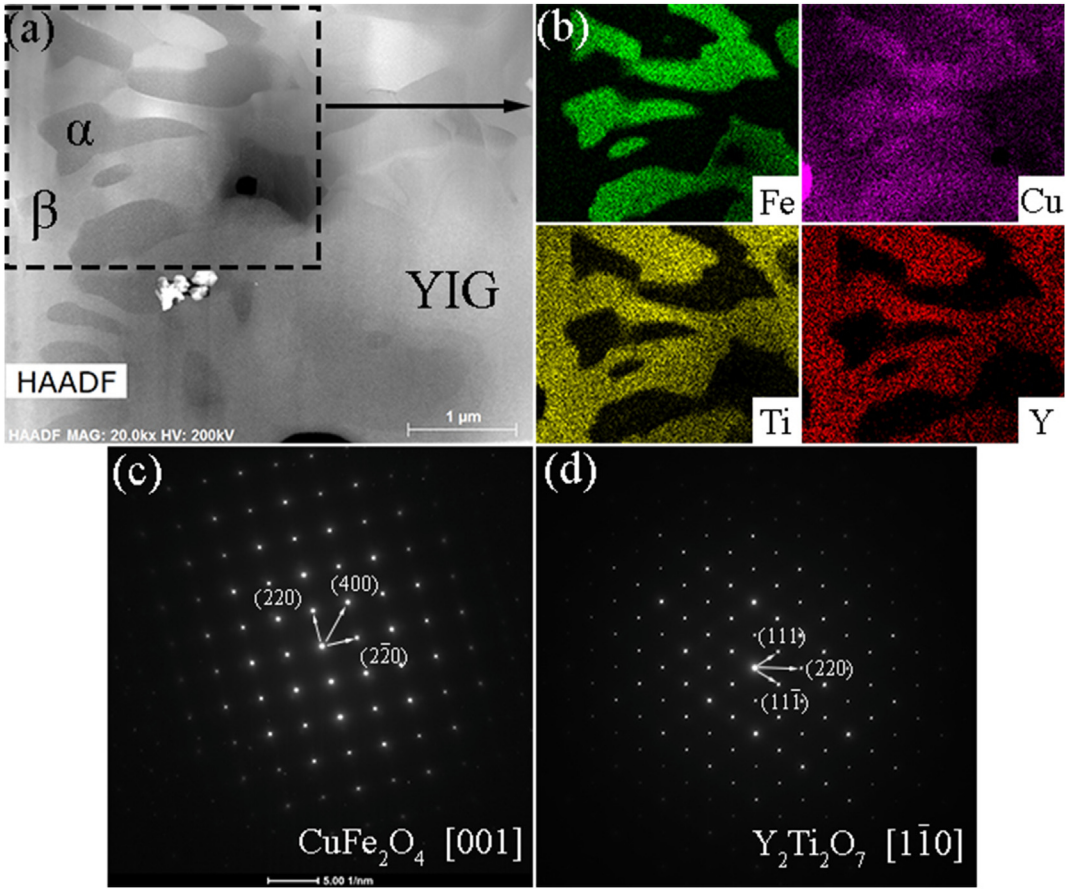

Fig. 13 – (a) Bright field image of the reaction layer formed adjacent to YIG ceramic; (b) Elements maps analysis of selected area marked with the black box in (a); (c) (d) SAED patterns of α and β in (a).

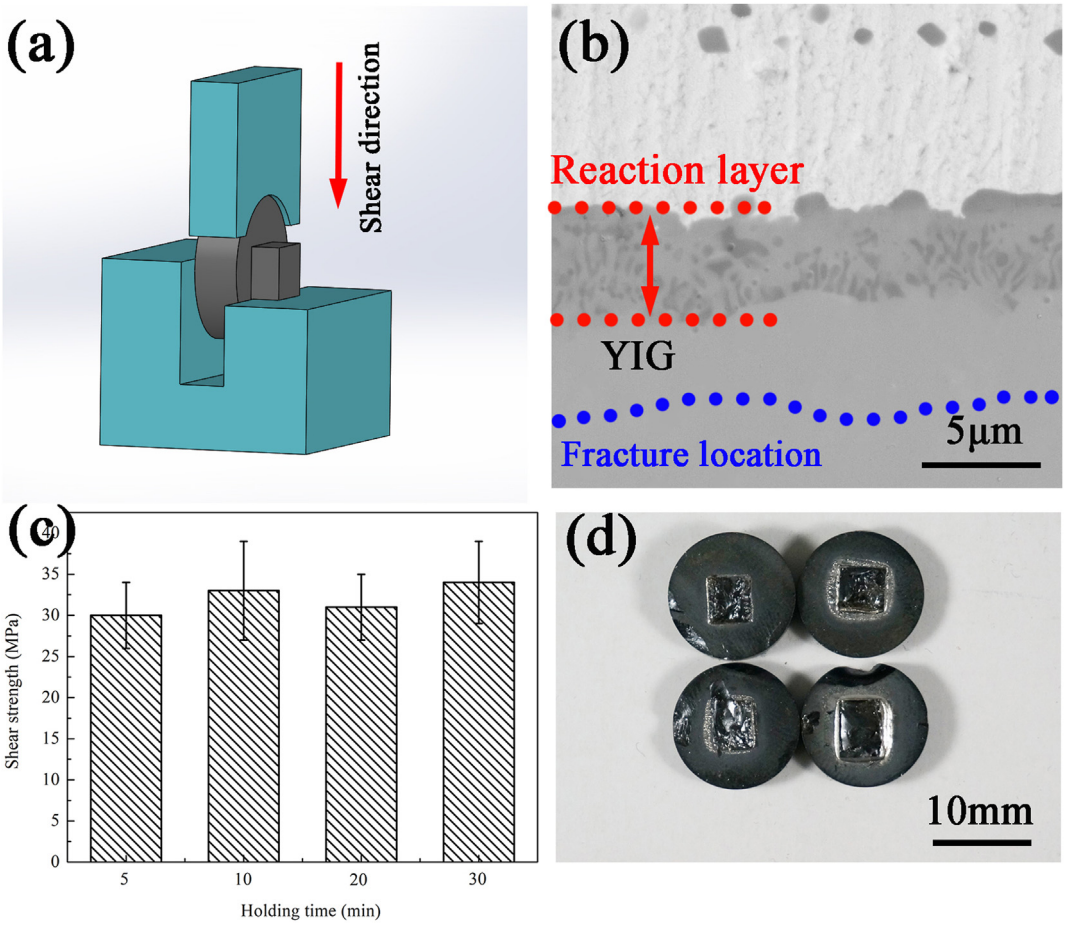

Fig. 14 – Shearing test on the joints brazed by Ag–8CuO–2TiO_2: (a) the schematic of the shearing test; (b) the schematic of fracture location; (c) the shear strength vs different holding time; (d) the optical images of some fracture samples.

interface after the addition of TiO_2. The strengths of the interfaces were characterized via nanoindentation. As shown in Fig. 15, the TiO_2-doped interface is harder than the Ag–10CuO interface, which is attributed to the dispersion strengthening of the $CuFe_2O_4$ that is dotted among $Y_2Ti_2O_7$. Due to the consumption of CuO during the reaction, the interface is free from the continuous intermetallic compound, which eliminates the source of cracks under the stress field. The joining scheme of Ag–8CuO–2TiO_2 is presented in Fig. 15. When the temperature reaches approximately 940 °C, the filler melts rapidly due to the eutectic reactions, namely, Ag+CuO and CuO+TiO_2. Then, CuO and TiO_2 drastically react with YIG to form a continuous reaction layer, which consists of a base, namely, $Y_2Ti_2O_7$, that is dotted with $CuFe_2O_4$. The introduction of Ti into $Y_2Ti_2O_7$ changes the characteristics of the YIG surface from passive to active, which renders the wetting process independent of CuO deposition. The contact angle decreases and stabilizes rapidly, in contrast to that of Ag–10CuO.

$CuFe_2O_4$ was most likely the transition phase of the solid reaction. This reaction is controlled by the short-range diffusion and interface reaction in the early stage of the process. Then, $CuFe_2O_4$ decomposes following long-range diffusion of Cu into the YIG substrate. The relationship between the decomposition of $CuFe_2O_4$ and intergranular penetration has not been elucidated. To the best of our knowledge, no study has been conducted on the influence of TiO_2 on the intergranular melting of YIG ceramics. The Ag–CuO–TiO_2 filler tends to penetrate into the Al_2O_3 ceramic. This phenomenon has been widely investigated. The addition of TiO_2 lowers the eutectic temperature of the CuO–Al_2O_3 system, which enables local melting along the grain boundaries [18]. The infiltration of the Ag–CuO–TiO_2 filler appears to be greater at a higher TiO_2/CuO ratio. The elements that are added during ceramic sintering, which are used to reduce the sintering temperature, may cause dissolution of the grain boundaries [22]. No other elements in addition to Y, Fe and O could be identified within the YIG ceramic via EDS analysis. Hence, it is possible that TiO_2 facilitates the reaction between CuO and YIG, which promotes the displacement of Fe and the formation of $CuFe_2O_4$. The promotion of the formation of $CuFe_2O_4$ could be proven by the $CuFe_2O_4$ band at the wetting frontier, as shown in Fig. 8c. When Cu diffuses into the YIG substrate, Ag penetrates along the grain boundaries with a low melting point. The eutectic reaction between Ag and Cu occurs in the penetration region. This finding suggests that robust joining between the Ag–CuO brazing filler and the YIG ceramic can be realized via the addition of TiO_2 to produce higher wettability and a stronger interface.

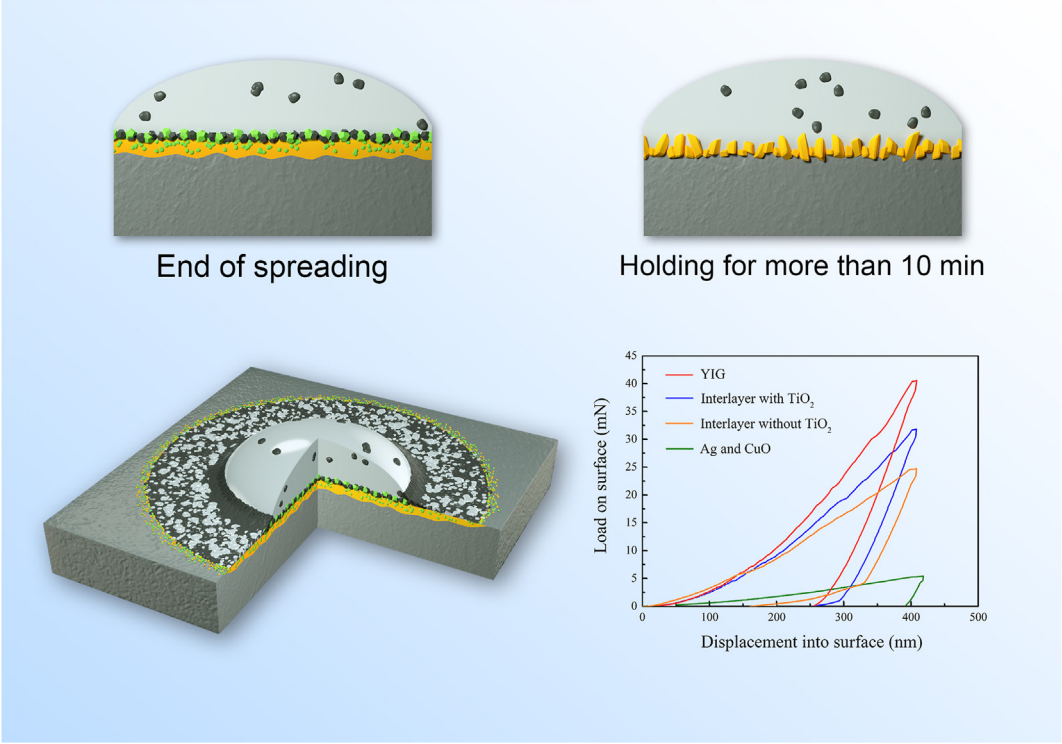

Fig. 15 – Illustration for joining schematics and mechanical property of the Ag–8CuO–2TiO_2.

4. Conclusions

The Ag–CuO filler shows enhanced wettability on a YIG ceramic substrate with the addition of TiO_2, associated with a final contact angle of 31° at 1000 °C, in comparison to the Ag–10CuO filler. When 2 at.% TiO_2 is added to the filler, a continuous reaction layer of $Y_2Ti_2O_7$ that is dotted with $CuFe_2O_4$ forms along the interface, which changes the inert YIG surface into an active reacted surface. The spreading of the Ag–8CuO–2TiO_2 filler no longer depends on the dissolution of CuO into the liquid. The YIG ceramics were joined successfully by an Ag–8CuO–2TiO_2 filler at 1000 °C for various holding times. The average shear strength exceeded 30 MPa in all cases with fractures at the ceramic side adjacent to the seam. The strengths of the interfaces were characterized via nanoindentation. The TiO_2-doped interface was harder than that of Ag–10CuO, which is attributed to the dispersion strengthening of the $CuFe_2O_4$ that was dotted among $Y_2Ti_2O_7$.

Data availability statement

The raw/processed data required to reproduce these findings cannot be shared at this time due to technical limitations.

Declaration of Competing Interest

The authors declare that they have no known competing financial interests or personal relationships that could have appeared to influence the work reported in this paper.

Acknowledgements

The authors acknowledge the financial support from the National Natural Science Foundation of China (Grant number: 51805115 and 51975150), and the China Postdoctoral Science Foundation (Project number: 2019M651280).

REFERENCES

[1] Bahadur D. Current trends in applications of magnetic ceramic materials. Bull Mater Sci 1992;15:431–9.
[2] Nan CW, Bichurin MI, Dong SX, Viehland D, Srinivasan G. Multiferroic magnetoelectric composites: historical perspective, status, and future directions. J Appl Phys 2008;103:1–35.
[3] Ganne JP, Lebourgeois R, Paté M, Dubreuil D, Pinier L, Pascard H. The electromagnetic properties of Cu-substituted garnets with low sintering temperature. J Eur Ceram Soc 2007;27:2771–7.
[4] Adam JD, Davis LE, Dionne GF, Schloemann EF, Stitzer SN. Ferrite devices and materials. IEEE Trans Microw Theory 2002;50:721–37.
[5] Chen YF, Wu KT, Yao YD, Peng CH, You KL, Tse WS. The influence of Fe concentration on $Y_3Al_{5-x}Fe_x O_{12}$ garnets. Microelectron Eng 2005;81:329–35.
[6] Niyaifar M, Ramani, Radhakrishna MC, Mozaffari M, Hasapour A, Amighian J. Magnetic studies of $Bi_xY_{3-x}Fe_5O_{12}$, fabricated using conventional method. Hyperfine Interact 2008;187:137–41.
[7] Cheng Z, Yang H, Yu L, Xu W. Saturation magnetic properties of $Y_{3x}Re_xFe_5O_{12}$ (Re: Gd, Dy, Nd, Sm and La) nanoparticles

grown by a sol–gel method. J Mater Sci Mater Electron 2008;19:442–7.
[8] Lira-Hernández IA, Sánchez-De Jesús F, Cortés-Escobedo CA, Bolarín-Miró AM. Crystal structure analysis of calcium-doped lanthanum manganites prepared by mechanosynthesis. J Am Ceram Soc 2010;93:3474–7.
[9] Ghosh S, Keyvavinia S, Roy WV, Mizumoto T, Roelkens G, Baets R. Ce:YIG/Silicon-on-Insulator waveguide optical isolator realized by adhesive bonding. Opt Express 2012;20:1839–48.
[10] Ghosh S, Keyvaninia S, Roy WV, Mizumoto T, Roelkens G, Baets R. Adhesively bonded Ce:YIG/SOI integrated optical circulator. Opt Lett 2013;38:965–7.
[11] Wang JG, Jiang N, Jiang HY. The high-temperatures bonding of graphite/ceramics by organ resin matrix adhesive. Int J Adhes Adhes 2006;26:532–6.
[12] Li J, Luo RY, Bi YH, Xiang Q, Lin C, Zhang YF, et al. The preparation and performance of short carbon fiber reinforced adhesive for bonding carbon/carbon composites. Carbon 2008;46:1957–65.
[13] Weil KS, Kim JY, Hardy JS. Reactive air brazing: a novel method of sealing SOFCs and other solid-state electrochemical devices. Electrochem Solid-State Lett 2005;8:A133–6.
[14] Friant JR, Meier A, Darsell JT, Weil KS. Transitions in wetting behavior between liquid Ag-CuO alloys and Al_2O_3 substrates. J Am Ceram Soc 2012;95:1549–55.
[15] Erskine KM, Meier AM, Joshi VV, Pilgrim SM. The effect of braze interlayer thickness on the mechanical strength of alumina brazed with Ag–CuO braze alloys. Adv Eng Mater 2014;16:1442–7.
[16] Sinnamon KE, Meier AM, Joshi VV. Wetting and mechanical performance of zirconia brazed with silver/copper oxide and silver/vanadium oxide alloys. Adv Eng Mater 2015;16:1482–9.
[17] Raju K, Muksin, Kim S, Song K, Yu JH, Yoon GH. Joining of metal-ceramic using reactive air brazing for oxygen transport membrane applications. Mater Des 2016;109:233–41.
[18] Weil KS, Jin YK, Hardy JS, Darsell JT. The effect of TiO_2 on the wetting behavior of silver–copper oxide braze filler metals. Scripta Mater 2006;54:1071–5.
[19] Hardy JS, Kim JY, Thomsen EC, Weil KS. Improved wetting of mixed ionic/electronic conductors used in electrochemical devices with ternary air braze filler metals. J Electrochem Soc 2007;154:P32–9.
[20] Lu FH, Fang FX, Chen YS. Eutectic reaction between copper oxide and titanium dioxide. J Eur Ceram Soc 2001;21:1093–9.
[21] Eustathopoulos N, Nicholas MG, Drevet B. Wettability at high temperatures. 1999. Pergamon, Amsterdam.
[22] Bettinelli A, Guille J, Bernier JC. Densification of alumina at 1400°C. Ceram Int 1988;14:31–4.
[23] Bridges D, Ma CL, Zhang SH, Xue SB, Feng ZL, Hu AM. Diffusion and wetting behaviors of Ag nanoparticle and Ag nanowire pastes for laser brazing of Inconel 718. Weld World 2018;62:169–76.